

Supersymmetric Exotic Decays of the 125 GeV Higgs Boson

Jinrui Huang,¹ Tao Liu,² Lian-Tao Wang,^{3,4} and Felix Yu⁵

¹Theoretical Division, T-2, MS B285, Los Alamos National Laboratory, Los Alamos, NM 87545, USA

²Department of Physics, The Hong Kong University of Science and Technology, Clear Water Bay, Kowloon, Hong Kong

³Enrico Fermi Institute, University of Chicago, Chicago, IL 60637, USA

⁴KICP and Dept. of Physics, University of Chicago, 5640 S. Ellis Ave., Chicago, IL 60637, USA

⁵Theoretical Physics Department, Fermi National Accelerator Laboratory, P. O. Box 500, Batavia, IL 60510, USA

We reveal a set of novel decay topologies for the 125 GeV Higgs boson in supersymmetry which are initiated by its decay into a pair of neutralinos, and discuss their collider search strategies. This category of exotic Higgs decays are characterized by the collider signature: visible objects + \cancel{E}_T , with \cancel{E}_T dominantly arising from escaping dark matter particles. Their benchmark arises naturally in the Peccei-Quinn symmetry limit of the MSSM singlet-extensions, which is typified by the co-existence of three light particles: singlet-like scalar h_1 and pseudoscalar a_1 , and singlino-like neutralino χ_1 , all with masses of $\lesssim 10$ GeV, and the generically suppression of the exotic decays of the 125 GeV Higgs boson $h_2 \rightarrow h_1 h_1$, $a_1 a_1$ and $\chi_1 \chi_1$, however. As an illustration, we study the decay topology: $h_2 \rightarrow \chi_1 \chi_2$, where the bino-like χ_2 decays to $h_1 \chi_1$ or $a_1 \chi_1$, and $h_1/a_1 \rightarrow f\bar{f}$, with $f\bar{f} = \mu^+ \mu^-$, $b\bar{b}$. In the di-muon case ($m_{h_1/a_1} \sim 1$ GeV), a statistical sensitivity of $\frac{S}{\sqrt{B}} > 6\sigma$ can be achieved easily at the 8 TeV LHC, assuming $\frac{\sigma(pp \rightarrow Wh_2)}{\sigma(pp \rightarrow Wh_{SM})} \text{Br}(h_2 \rightarrow \mu^+ \mu^- \chi_1 \chi_1) = 0.1$. In the $b\bar{b}$ case ($m_{h_1/a_1} \sim 45$ GeV), 600 fb⁻¹ data at the 14 TeV LHC can lead to a statistical sensitivity of $\frac{S}{\sqrt{B}} > 5\sigma$, assuming $\frac{\sigma(pp \rightarrow Zh_2)}{\sigma(pp \rightarrow Zh_{SM})} \text{Br}(h_2 \rightarrow b\bar{b} \chi_1 \chi_1) = 0.5$. These exotic decays open a new avenue for exploring new physics couplings with the 125 GeV Higgs boson at colliders.

[Introduction] The discovery of a 125 GeV Higgs resonance at the CMS [1] and ATLAS [2] experiments has launched an era of precision Higgs phenomenology, emphasizing CP and spin discrimination and exotic Higgs decays. Of particular interest are exotic Higgs decays that arise in well-motivated new physics (NP) scenarios aimed at solving the gauge hierarchy problem by stabilizing the Higgs mass against divergent quantum corrections, such as supersymmetry (SUSY). The Higgs mass stabilization mechanism generally manifests itself through Higgs couplings absent in the Standard Model (SM). The 125 GeV Higgs therefore is expected to be a leading window into NP.

Because the 125 GeV SM Higgs decay width is small ($\Gamma \sim 4$ MeV), a new coupling between the Higgs boson and some light particles may lead to a large exotic Higgs decay branching fraction. The current bounds on such channels are still weak: a branching fraction as large as $\sim 60\%$ is allowed at the 2σ C.L. [3–7], in a general context, e.g., if new physics is allowed to enter the Higgs-gluon-gluon coupling. If SM couplings are assumed, theorist-performed fits constrain the invisible branching fraction to be $\lesssim 25\%$ at 95% C.L. [3, 4]. Even with the full 300 fb⁻¹ of the 14 TeV LHC, the projected upper bound is $\sim 10\%$ at the 2σ C.L. on such channels [8] (mainly driven by estimates of systematic errors), which still leaves appreciable room for an exotic decay mode. Searches for exotic decays are therefore very natural and effective tools to explore possible and exciting new couplings to the 125 GeV Higgs boson.

Exotic Higgs decays are often grouped into two categories according to their collider signatures: (1) purely \cancel{E}_T ; (2) visible objects (no \cancel{E}_T , except for neutrinos from

heavy quark or tau decays). Case (1) is mainly dark matter (DM) motivated and was originally studied in [9]. A well-known example for case (2) is the R -symmetry limit of the Next-to-Minimal Supersymmetric Standard Model (NMSSM) [10], in which the SM-like Higgs can significantly decay to a pair of light singlet-like R -axions (a_1).

Separately, there is the deep cosmic mystery of DM. In the past decade, a few DM direct detections have reported excesses, which can controversially be interpreted as hints of a sub-electroweak (EW) scale DM particle with a relatively large spin-independent direct detection cross section [11–14]. One of the most interesting possibilities arises from the approximate Peccei-Quinn (PQ) symmetry limit in the NMSSM [15, 16]. In this scenario, the lightest neutralino is singlino-like and has a mass of $\lesssim 10$ GeV, providing a naturally light DM candidate. Moreover, pair annihilation into the light pseudoscalar as well as exchange of the light scalar with nucleons allow the singlino to achieve simultaneously the correct relic density and the large direct detection cross section indicated by some experiments [15].

In this letter we will note that the PQ-symmetry limit not only provides a supersymmetric benchmark for sub-EW scale DM, but we also emphasize its very rich Higgs physics. The phenomenology is characterized by new SM-like Higgs (h_2) exotic decays: $h_2 \rightarrow \chi_1 \chi_2, \chi_2 \chi_2$, with the subsequent decays $\chi_2 \rightarrow h_1 \chi_1, a_1 \chi_1$ and h_1, a_1 into SM particles (here χ_1 and χ_2 are the lightest and the second lightest neutralinos, respectively). The PQ-symmetry limit therefore provides benchmarks for a third category of exotic Higgs decays: (3) visible objects and \cancel{E}_T , where \cancel{E}_T dominantly arises from DM candidates.

[Theoretical Motivations] To address the notorious

μ problem in the MSSM, various singlet-extensions of the MSSM have been explored, such as the NMSSM [17] and the nearly-MSSM (nMSSM) [18], where different symmetries are introduced to forbid the bare μ term in the MSSM. These models share a common global PQ-symmetry limit [19], with the superpotential and soft SUSY-breaking terms given by

$$\begin{aligned} \mathbf{W} &= \lambda \mathbf{S} \mathbf{H}_u \mathbf{H}_d + \mathcal{O}(\kappa) , \\ V_{\text{soft}} &= m_{H_d}^2 |H_d|^2 + m_{H_u}^2 |H_u|^2 + m_S^2 |S|^2 \\ &\quad - (\lambda A_\lambda H_u H_d S + \text{h.c.}) + \mathcal{O}(\kappa) , \end{aligned} \quad (1)$$

where H_d , H_u and S are the neutral fields of the \mathbf{H}_d , \mathbf{H}_u and \mathbf{S} superfields, respectively. Small explicit PQ-breaking terms (denoted by $\mathcal{O}(\kappa)$), such as $\kappa \mathbf{S}^3$ and its softly SUSY breaking term $A_\kappa \kappa \mathbf{S}^3$ in the NMSSM, are surely allowed in realistic scenarios. Once the singlet scalar S obtains a vacuum expectation value (VEV) $\langle S \rangle = v_S$, an effective μ parameter $\mu = \lambda v_S$ can be generated. Since the current LHC data constrains large mixing between the CP -even and CP -odd Higgs sector [5, 20], we assume no CP -violation in the Higgs sector.

One feature of this scenario is that in the decoupling limit ($\lambda = \frac{\mu}{v_S} \lesssim \mathcal{O}(0.1)$), the lightest CP -even (h_1), CP -odd (a_1) Higgs bosons and the lightest neutralino (χ_1) form an approximate singlet-like PQ-axion supermultiplet. These states, mainly the saxion, axion, and axino, respectively, are much lighter than the PQ-symmetry breaking scale. This is because the PQ symmetry breaking is mainly controlled by the singlet superfield \mathbf{S} in this scenario, while the mass splittings among the saxion, axion and axino are induced by SUSY breaking and are suppressed (recall, if SUSY is unbroken, their masses are degenerate). Explicitly, $m_{h_1}^2$, m_{χ_1} are given by

$$\begin{aligned} m_{h_1}^2 &= -4v^2 \varepsilon^2 + \frac{4\lambda^2 v^2}{\tan^2 \beta} \left(1 - \frac{\varepsilon m_Z}{\lambda \mu} \right) \left(1 + \frac{2\varepsilon \mu}{\lambda m_Z} \right) \\ &\quad + 16 \frac{v^4}{m_Z^2} \varepsilon^4 + \sum_{i=0}^5 \mathcal{O} \left(\frac{\lambda^{5-i}}{\tan^i \beta}, \kappa \right) , \\ m_{\chi_1} &= -\frac{\lambda^2 v^2 \sin 2\beta}{\mu} + \sum_{i=0}^5 \mathcal{O} \left(\frac{\lambda^{5-i}}{\tan^i \beta}, \kappa \right) , \end{aligned} \quad (2)$$

with $\varepsilon = \frac{\lambda \mu}{m_Z} \varepsilon'$, $\varepsilon' = \left(\frac{A_\lambda}{\mu \tan \beta} - 1 \right)$. Avoiding a tachyonic h_1 mass immediately requires

$$\varepsilon^2 < \frac{\lambda^2}{\tan^2 \beta} + \text{loop corrections} . \quad (3)$$

This constraint has important implications for the decay of the SM-like Higgs. Note the contribution of $Z \rightarrow \chi_1 \chi_1$ to the Z invisible decay width is small, because the non-singlino content in χ_1 is of the order $\lambda v/\mu$, and the $Z \chi_1 \chi_1$ coupling is suppressed by $(\lambda v/\mu)^2$, where $v = 174$ GeV.

Though kinematically allowed, the decays of the SM-like Higgs $h_2 \rightarrow a_1 a_1$, $h_1 h_1$ are suppressed in the PQ-symmetry limit. The tree-level couplings of the SM-like

Higgs boson h_2 with $h_1 h_1$ and $a_1 a_1$ are

$$\begin{aligned} y_{h_2 a_1 a_1} &= -\sqrt{2} \lambda \varepsilon \frac{m_Z v}{\mu} + \sum_{i=0}^4 \mathcal{O} \left(\frac{\lambda^{4-i}}{\tan^i \beta}, \kappa \right) , \\ y_{h_2 h_1 h_1} &= -\sqrt{2} \lambda \varepsilon \frac{m_Z v}{\mu} + 2\sqrt{2} \varepsilon^2 v + \sum_{i=0}^4 \mathcal{O} \left(\frac{\lambda^{4-i}}{\tan^i \beta}, \kappa \right) , \end{aligned} \quad (4)$$

both of which are suppressed by $|\lambda \varepsilon| \ll 1$. Unlike the R -symmetry limit of the NMSSM (defined by $A_{\lambda, \kappa} \rightarrow 0$), these decay channels are therefore rather inconsequential for the SM-like Higgs in our scenario.

In the PQ-symmetry limit, however, the SM-like Higgs has a significant decay width into a pair of neutralinos $h_2 \rightarrow \chi_1 \chi_2$, $\chi_2 \chi_2$, if kinematically allowed. Since χ_1 is light, $h_2 \rightarrow \chi_1 \chi_2$ can be significant, *e.g.*, if χ_2 is binolike, with $m_{\chi_2} \lesssim 100$ GeV (note $h_2 \rightarrow \chi_2 \chi_2$ is also possible but tends to be phase-space suppressed), while $h_2 \rightarrow \chi_1 \chi_1$ is suppressed by the small mixing angle of the singlino-like χ_1 . Their relative strength can be understood via the couplings

$$y_{h_2 \chi_1 \chi_2} \sim \mathcal{O} \left(\frac{\lambda g_1 v}{\mu} \right) , \quad y_{h_2 \chi_1 \chi_1} \sim \mathcal{O} \left(\frac{\lambda^2 v}{\mu \tan \beta} \right) . \quad (5)$$

The decay width $\Gamma_{h_2 \rightarrow \chi_1 \chi_2}$ therefore is typically larger than $\Gamma_{h_2 \rightarrow \chi_1 \chi_1}$. Given that $\Gamma_{h \rightarrow b\bar{b}}$ is dictated by the coupling $\frac{m_b}{\sqrt{2}v}$, $\text{Br}(h_2 \rightarrow \chi_1 \chi_2)$ can be sizable, as shown in Fig. 1, and even larger than the partial widths to SM final states. The χ_2 dominantly decays into $\chi_1 a_1$ or $\chi_1 h_1$, which are usually the only kinematically accessible channels. Therefore, the PQ-symmetry limit of the MSSM singlet-extensions provides new supersymmetric decay topologies for the SM-like Higgs boson, including the one shown in Fig. 2, which we now discuss in detail.

[LHC Studies] The branching fractions of h_1 and a_1 (we do not distinguish h_1 and a_1 below) into the SM fermions $f\bar{f}$ are highly sensitive to their masses. The decay products $f\bar{f}$ tend to be soft, because of the restricted phase space, and to be collimated: their characteristic angular separation $\Delta R \equiv \sqrt{(\Delta\eta)^2 + (\Delta\phi)^2} \sim 2m_{h_1}/p_{T, h_1}$ is small since typically $m_{h_1} \ll p_{T, h_1}$, where $\Delta\eta$ and $\Delta\phi$ are the differences in pseudorapidity and azimuthal angle of $f\bar{f}$, respectively. Our new exotic Higgs decay collider signature is therefore $f\bar{f} + \cancel{E}_T + X$, where $f\bar{f}$ behaves as lepton-jet(s) or jet(s), and X denotes the particles associated with the h_2 production. Two benchmarks, with $f\bar{f} = \mu^+ \mu^-$ and $b\bar{b}$, respectively, are listed in Table I. Another interesting possibility is $f\bar{f} = \tau^+ \tau^-$ which is challenging, however, because of the failure of the standard tau identification method due to the softness and collimation of the $\tau^+ \tau^-$ signal. Thus, extracting the ditau signal requires a sophisticated treatment of backgrounds, exemplified by QCD and soft tracks. We will present the relevant sensitivity analysis in [22].

To design the collider strategies which can optimally cover the full space of models, we perform the analysis

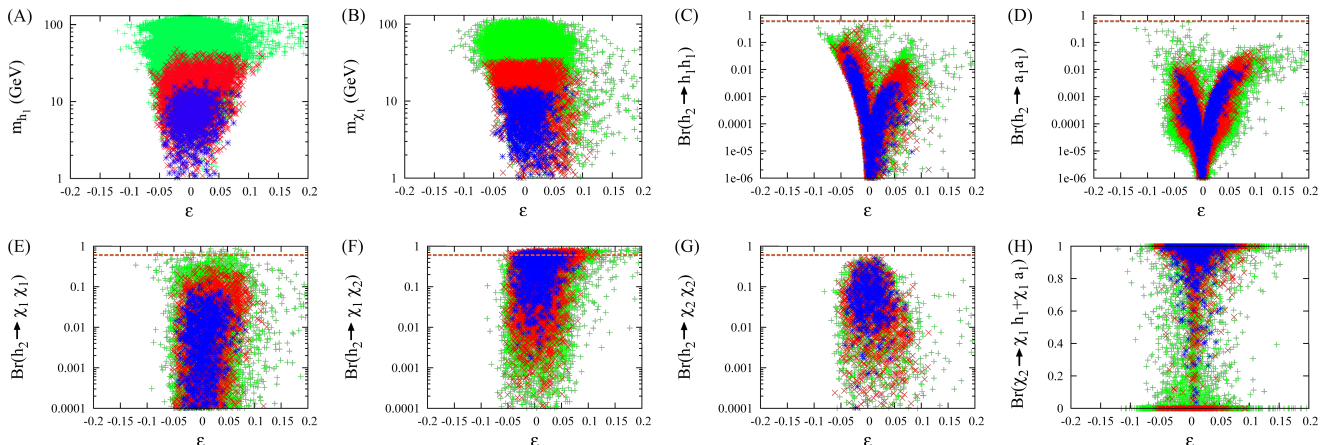


FIG. 1: Masses of (A) h_1 and (B) χ_1 ; branching ratios of h_2 into (C) $h_1 h_1$, (D) $a_1 a_1$, (E) $\chi_1 \chi_1$, (F) $\chi_1 \chi_2$, (G) $\chi_2 \chi_2$ and (H) χ_2 into $\chi_1 h_1$ and $\chi_1 a_1$, in the PQ-symmetry limit of the NMSSM. Points are sampled in the ranges $3 \leq \tan \beta \leq 30$, $0.015 \leq \lambda \leq 0.5$, $0.0005 \leq \kappa \leq 0.05$, $-0.8 \leq \epsilon' \leq 0.8$, $-50 \text{ GeV} \leq A_\kappa \leq 0$, and $0.1 \text{ TeV} \leq \mu \leq 1 \text{ TeV}$. We have assumed soft squark masses of 2 TeV, slepton masses of 200 GeV, $A_{u,d,e} = -3.5 \text{ TeV}$, and bino, wino and gluino masses of 30-120, 150-500 and 2000 GeV, respectively. Green (light gray) points cover the whole scan range, red (medium gray) points correspond to $\lambda < 0.30$, $\kappa/\lambda < 0.05$ and $\mu < 350 \text{ GeV}$, and blue (dark gray) points correspond to $\lambda < 0.15$, $\kappa/\lambda < 0.03$ and $\mu < 250 \text{ GeV}$. In addition to the regular LEP, Tevatron and LHC bounds set in NMSSTools 3.1.0 [21], we require m_{h_2} to be within 124 – 126 GeV. The dashed orange line in (C-G) depicts a 60% exotic Higgs decay limit allowed at 2σ C.L. [3–7] (see main text).

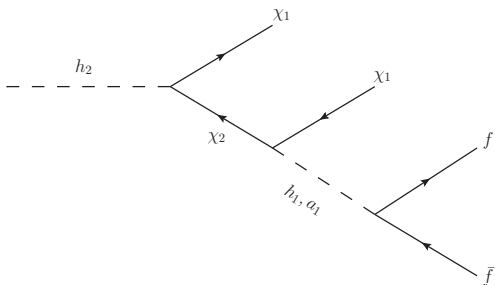


FIG. 2: A new decay topology of the SM-like Higgs boson.

	m_{h_1}	m_{h_2}	m_{χ_1}	m_{χ_2}
$h_1 \rightarrow \mu^+ \mu^-$	1 GeV	125 GeV	10 GeV	80 GeV
$h_1 \rightarrow b\bar{b}$	45 GeV			

TABLE I: Two benchmarks used for the collider analyses.

model-independently and introduce a rescaling factor

$$c_{\text{eff}} = \frac{\sigma(pp \rightarrow h_2)}{\sigma(pp \rightarrow h_{\text{SM}})} \times \text{Br}(h_2 \rightarrow \chi_1 \chi_2) \quad (6)$$

$$\times \text{Br}(\chi_2 \rightarrow h_1 \chi_1) \times \text{Br}(h_1 \rightarrow f \bar{f}),$$

where $\sigma(pp \rightarrow h_2, h_{\text{SM}})$ are the production cross sections for the SM-like and SM Higgs in the relevant production mode, and we assume the narrow width approximation for each intermediate decaying particle. Given the absence of dedicated collider searches so far, the current upper bound for c_{eff} is from fitting the results of standard Higgs searches, and hence is not sensitive to m_{h_1} .

The samples for both analyses are simulated using MadGraph 5 [23] with CTEQ6L1 parton distribution functions [24] and, for the $h_1 \rightarrow b\bar{b}$ benchmark, MLM

matching [25, 26]. They are showered and hadronized using PYTHIA v6.4.20 [27]. For the $\mu^+ \mu^-$ case, we use PGS v4 [28] for basic detector simulation. For the $b\bar{b}$ case, since we will perform a jet substructure analysis, we use a more sophisticated mock detector simulation based on physics object studies performed by ATLAS and CMS for jets [29], electrons [30], muons [31], and \cancel{E}_T [32].

[Case I: $h_2 \rightarrow \mu^+ \mu^- + \cancel{E}_T$] For $m_{h_1} \lesssim 1 \text{ GeV}$, the dominant decay channel is $h_1 \rightarrow \mu^+ \mu^-$, resulting in $\Delta R_{\mu^+ \mu^-} \sim 0.1$ for the benchmark point in Table I. These muons generally fail the usual isolation requirements in multilepton SUSY searches (where summing over all particles' p_T in the cone around each muon is typically assumed), rendering such searches insensitive to this channel. In addition, though searches for lepton-jets at the LHC [33–35] do not impose isolation requirements on the collimated leptons, they make additional requirements which render them insensitive to our model. Namely, these searches require a displaced vertex for the lepton-jet [33], at least four muons within a single lepton-jet [34], or at least two lepton-jets [34, 35]: all of these features are absent in this scenario. The most sensitive search comes from Ref. [36], which used 35 pb^{-1} of 7 TeV data to search for resonances decaying to muon pairs. After applying their analysis cuts, we obtain a signal cross section of $\sigma(gg \rightarrow h)_{\text{SM}} \times c_{\text{eff}} \times A \sim 0.1 \text{ pb} \times c_{\text{eff}}$, which well satisfies their 0.15 – 0.7 pb limit for masses below 1 GeV [36].

We now proceed with developing a collider analysis for identifying the dimuon signal in our model. As an illustration, we focus on the Wh_2 mode with the W decaying leptonically ($\ell = e, \mu$). The muons from the h_1 decay

are collimated, and so we define a new muon isolation cut, which requires the particle p_T sum (excluding the nearby-muon contribution) in the $\Delta R < 0.4$ cone around each muon candidate to be $p_{T,iso}(\mu^\pm) < 5$ GeV. This can efficiently discriminate the h_1 muons and the ones from semi-leptonic meson decays. The main background then arises from $W\gamma^*/Z^* \rightarrow \ell\nu\mu^+\mu^-$. We assume a tri-lepton trigger in the analysis. Alternatively, we could have triggered on the single lepton from the W decay, which would not significantly alter our conclusions.

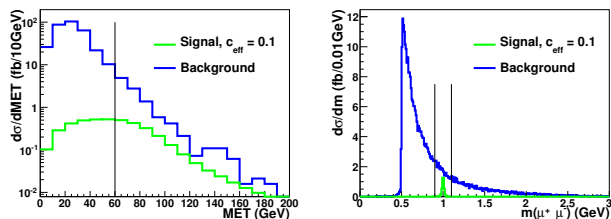


FIG. 3: Differential cross section vs. E_T (left) and $m_{\mu^+\mu^-}$ (right) at the 8 TeV LHC. We have applied basic acceptance cuts to both signal (choosing $c_{\text{eff}} = 0.1$) and background and additional cut of $m_{\mu^+\mu^-} \geq 0.5$ GeV to the background to ensure efficient Monte Carlo (MC) generation. The black line indicates the cuts $E_T > 60$ GeV and $0.9 < m_{\mu^+\mu^-} < 1.1$ GeV, respectively.

Cuts and Efficiencies	Wh_2	$W(\gamma^*/Z \rightarrow \mu^+\mu^-)$
Cross section (pb)	$0.149 \times c_{\text{eff}}$	26.6
Lepton geometric, p_T , and isolation requirements	28.2%	1.22%
$E_T \geq 60$ GeV	12.5%	0.0403%
$0.9 \leq m_{\mu^+\mu^-} \leq 1.1$ GeV	12.3%	0.0047%
$S, B, \frac{S}{\sqrt{B}}$ ($20 \text{ fb}^{-1}, c_{\text{eff}} = 0.1$)	37, 32, 6.5σ	

TABLE II: Analysis cuts (see main text) and efficiencies at the 8 TeV LHC for the $h_1 \rightarrow \mu^+\mu^-$ channel. The decay $W \rightarrow \ell\nu$, $\ell = e, \mu$ is assumed in the quoted cross section, and a K -factor of 1.3 is included for the background.

In Fig. 3, we show the E_T and $m_{\mu^+\mu^-}$ distributions after imposing basic acceptance cuts at the 8 TeV LHC. Namely, we require $|\eta_\ell| \leq 2.4$ for all charged leptons, $\Delta R_{\mu^+\mu^-} < 0.2$ and $p_{T,\mu} \geq 10$ GeV for candidate h_1 muon pairs, and $p_{T,\ell} \geq 20$ GeV for a third lepton. We also impose the new muon isolation requirement detailed above. The complete cut efficiency is presented in Table II. With 20 fb^{-1} data, we can obtain a local statistical sensitivity $S/\sqrt{B} = 6.5\sigma$, with a typical value of $c_{\text{eff}} = 0.1$ (see discussions, e.g., in [37, 38]) assumed. A larger significance is certainly possible, though, if the $m_{\mu^+\mu^-}$ cut was tightened, or additional triggers were added. This dedicated analysis can be easily extended to the other possibilities, e.g. Zh_2 events. On the other hand, we have neglected the background resulting from jets and photons faking electrons and lost jets faking E_T , as well as subleading sources of fake muons. We expect all of these contribu-

tions arising from fakes to be subdominant compared to the irreducible $W\gamma^*/Z^*$ background.

[**Case II:** $h_2 \rightarrow b\bar{b} + E_T$] For $m_{h_1} > 10$ GeV, h_1 dominantly decays into a relatively soft $b\bar{b}$ pair. Unlike previous Higgs boson studies in the $b\bar{b}$ channel [39–41], the h_1 boson in our scenario results from the cascade decay of a $\mathcal{O}(100)$ GeV parent particle, imparting only a mild boost to the $b\bar{b}$ system. We will reconstruct the $h_1 \rightarrow b\bar{b}$ signal using jet substructure tools appropriately modified for non-boosted resonances. To avoid washing out our hadronic signal and because our E_T significance is not strong enough for a standalone trigger, we will focus on the Zh_2 mode and trigger on the leptonic Z decay. Then the dominant background is Z + heavy flavor jets.

We first aim to identify the Z candidate from its same flavor opposite sign (SFOS) e^+e^- or $\mu^+\mu^-$ decays, which can efficiently remove the $t\bar{t}$ background, then we find the b -tagged h_1 candidate jet and probe its substructure. We cluster jets using the angular-ordered Cambridge-Aachen algorithm [42, 43] from FASTJET v3.0.2 [44] with distance parameter $R = 1.2$. After applying the $E_T > 80$ GeV cut, we count the number of b -tagged jets with $p_T > 20$ GeV. Our b -tagging efficiency is 60% with a mistag rate 10% for c -jets and 1% for the other light jets. We choose to retain the 1 b -tag bin for the jet substructure analysis.

Having isolated the dilepton system as well as the cascade decay of the h_2 boson, we can apply an additional cut with the expectation that the dilepton system recoils against the collimated h_2 cascade decay. We construct the scalar sum p_T of the h_2 candidate, $p_T(h_2) = p_T(b\text{-jet}) + |E_T|$, and then divide it by the p_T of the dilepton system: $p_{T,\text{frac}} \equiv p_T(h_2)/p_T(\ell\ell_{\text{sys}})$. The $p_{T,\text{frac}}$ distribution is shown in Fig. 4. We observe that the cutting on $p_{T,\text{frac}}$ works well at reducing the $t\bar{t}$ background, where the E_T signal tends to arise from neutrinos of separate decay chains instead of a single cascade decay.

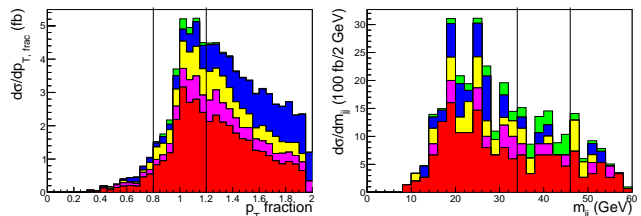


FIG. 4: Differential cross section vs. $p_{T,\text{frac}}$ (left) and m_{jj} (right), as defined in the text, after applying the Z mass window, E_T , and $N_{b\text{-tag}} = 1$ cuts (and $p_{T,\text{frac}}$ cut) at the 14 TeV LHC. Red is $Zb\bar{b}$ background, blue is $t\bar{t}$ background, magenta is the $Zc\bar{c}$ background, yellow is the $Zc+Z\bar{c}$ background and green is Zh_2 signal. The black vertical lines indicate the $p_{T,\text{frac}}$ window, $0.8 < p_{T,\text{frac}} < 1.2$, and the m_{jj} requirement in our analysis. We have set $c_{\text{eff}} = 0.5$.

Finally, we apply jet substructure techniques to investigate the kinematics of the b -tagged, $R = 1.2$ jet. Since we expect the Z + heavy flavor jets background to include more final state radiation than our $h_1 \rightarrow b\bar{b}$ signal,

Cut, efficiencies	Zh_2	Zbb	$Zc\bar{c}$	$Zc + Z\bar{c}$	$t\bar{t}$
Cross section (pb)	$0.09 \times c_{\text{eff}}$	48.4	32.8	139	41.8
Lepton cut	0.191	0.177	0.170	0.163	0.012
$\cancel{E}_T > 80$ GeV	8.31E-2	3.15E-3	4.41E-3	1.80E-3	4.57E-3
$N_{b\text{-tags}} = 1$, jet $p_T > 20$ GeV	3.78E-2	1.09E-3	4.88E-4	1.31E-4	1.86E-3
$0.8 < p_T, \text{frac} < 1.2$	2.59E-2	3.35E-4	1.06E-4	3.59E-5	7.70E-5
Two hardest subjets: $34 < m_{jj} < 46$ GeV	3.48E-3	7.17E-6	2.44E-6	5.00E-7	1.44E-6
$S, B, \frac{S}{\sqrt{B}}$ (600 fb $^{-1}$, $c_{\text{eff}} = 0.5$)	93, 208+48+42+36, 5.1 σ				

TABLE III: Analysis cuts and efficiencies at 14 TeV LHC for the $h_1 \rightarrow b\bar{b}$ channel. The standard cross section normalizations have been adopted: 833 pb for $t\bar{t}$ events [45], and 0.883 pb for Zh_2 events [46]. A K -factor of 1.3 is included for the other backgrounds. The decays $Z \rightarrow \ell^+\ell^-$ and, for top decays, $W \rightarrow \ell\nu$, $\ell = e, \mu, \tau$ are included in the quoted cross sections, where preselection cuts have been applied. The lepton cut requires the two hardest leptons ($\ell = e, \mu$) satisfy: SFOS, $p_T > 40$ GeV, $|m_{\ell\ell} - m_Z| < 10$ GeV.

we recluster the $R = 1.2$ jet using a smaller cone size of $R = 0.3$. We count the number of subjets with $p_T > 10$ GeV, and for events with two such subjets, we plot the invariant mass of the subjets in Fig. 4. We can readily observe a feature close to the $m_{h_1} = 45$ GeV mass in the data. Complete cut flow information and sensitivity calculation are presented in Table III. With 600 fb $^{-1}$ of 14 TeV LHC data, in the mass window of $34 < m_{jj} < 46$ GeV, the excess has a local significance of $S/\sqrt{B} = 5.1\sigma$, with $c_{\text{eff}} = 0.5$ assumed¹. The sensitivity could potentially be improved by further refining jet substructure techniques to tease out the soft h_1 signal subjets from the difficult hadronic collider environment, or choosing a new trigger such as vector boson fusion.

[Summary] In summary, the 125 GeV Higgs may be the leading window into NP, while its exotic decays provide a very natural and efficient way to explore such NP. The PQ-symmetry limit of the MSSM singlet-extensions provides a supersymmetric benchmark not only for a DM candidate at the sub-EW scale, but also for a third category of exotic decays of the 125 GeV Higgs (including both $h_2 \rightarrow \chi_1\chi_2$ and $h_2 \rightarrow \chi_2\chi_2$). This category of exotic Higgs decays are characterized by novel collider signatures - visible objects ($b\bar{b}, \tau^+\tau^-, l^+l^-$, lepton jets, γ , etc.) + \cancel{E}_T , and have rarely been considered before (though similar topologies may also arise in some neutrino models where the Higgs decays into two differ-

ent neutrinos with the heavier one further decaying via an off-shell gauge boson, e.g., see [48–50]; for different topologies with a fermions (jets)+ \cancel{E}_T signature, which may occur, e.g., in the multi-Higgs models with extra singlet, see [38] ([51])). This motivates new directions in exploring exotic Higgs decays at colliders, and also opens a new avenue to probe for new physics couplings with the 125 GeV Higgs boson.

Indeed, given their significant role as new physics probes, a systematic survey exploring exotic Higgs decays (including the other categories of collider signatures: (1) $h \rightarrow$ purely \cancel{E}_T and (2) $h \rightarrow$ visible objects) was pursued by ref [38]. The exotic Higgs decays with various topologies and collider signatures are prioritized according to their theoretical motivation and their experimental feasibility. Some highly motivated searches for the LHC are the channels proposed in this letter, $h_2 \rightarrow \chi_1\chi_2, \chi_2\chi_2$ with χ_2 further decaying leptonically. For more challenging cases, suggestions for improving their search sensitivities, i.e. via new triggers, are made. For more details in this regard, please see ref [38] or visit the website <http://exotichiggs.physics.sunysb.edu/web/wopr/>.

Acknowledgments

We would like to thank Brock Tweedie, Patrick Draper, Michael Graesser, Joe Lykken, Adam Martin, Jessie Shelton, Matt Strassler and Carlos Wagner for useful discussions. TL is supported by his start-up fund at the Hong Kong University of Science and Technology. JH is supported by the DOE Office of Science and the LANL LDRD program. JH would also like to thank the hospitality of University of Washington, where part of the work was finished. L-TW is supported by the DOE Early Career Award under Grant de-sc0003930. L-TW is also supported in part by the Kavli Institute for Cosmological Physics at the University of Chicago through NSF Grant PHY-1125897 and an endowment from the Kavli Foundation and its founder Fred Kavli. Fermilab is operated by the Fermi Research Alliance, LLC under Contract No. DE-AC02-07CH11359 with the US Department of Energy.

We also would like to acknowledge the hospitality of the Kavli Institute for Theoretical Physics and the Aspen Center for Physics, where part of this work was completed, and this research is supported in part by the National Science Foundation under Grant No. NSF PHY11-25915.

¹ A c_{eff} value as large as 0.5 usually requires new physics enter the Higgs-gluon-gluon coupling, otherwise the upper bound is about 0.25 at 95% C.L. [3, 4, 47]. While our model may potentially accommodate this requirement, studying the relevant physics is beyond the scope of this letter. Instead, we remark that the sensitivity for different c_{eff} values can be easily obtained via rescaling. Moreover, additional production modes for the Higgs, such as supersymmetric cascade decays, can have kinematics that readily overlap with our benchmark modes and effectively enhance c_{eff} .

- [1] S. Chatrchyan *et al.* [CMS Collaboration], Phys. Lett. B **716**, 30 (2012) [arXiv:1207.7235 [hep-ex]].
- [2] G. Aad *et al.* [ATLAS Collaboration], Phys. Lett. B **716**, 1 (2012) [arXiv:1207.7214 [hep-ex]].
- [3] G. Belanger, B. Dumont, U. Ellwanger, J. F. Gunion and S. Kraml, arXiv:1302.5694 [hep-ph].

- [4] P. P. Giardino, K. Kannike, I. Masina, M. Raidal and A. Strumia, arXiv:1303.3570 [hep-ph].
- [5] A. Djouadi and G. ég. Moreau, arXiv:1303.6591 [hep-ph].
- [6] [ATLAS Collaboration], ATLAS-CONF-2013-034.
- [7] [CMS Collaboration], CMS-PAS-HIG-13-005.
- [8] M. E. Peskin, arXiv:1207.2516 [hep-ph].
- [9] J. F. Gunion, Phys. Rev. Lett. **72**, 199 (1994) [hep-ph/9309216]. D. Choudhury and D. P. Roy, Phys. Lett. B **322**, 368 (1994) [hep-ph/9312347]; S. G. Frederiksen, N. Johnson, G. L. Kane and J. Reid, Phys. Rev. D **50**, 4244 (1994).
- [10] B. A. Dobrescu *et al.*, Phys. Rev. D **63**, 075003 (2001); B. A. Dobrescu and K. T. Matchev, JHEP **0009**, 031 (2000) [hep-ph/0008192]. R. Dermisek *et al.*, Phys. Rev. Lett. **95**, 041801 (2005). S. Chang, P. J. Fox and N. Weiner, JHEP **0608**, 068 (2006) [hep-ph/0511250]. S. Chang and N. Weiner, JHEP **0805**, 074 (2008) [arXiv:0710.4591 [hep-ph]]. P. W. Graham, A. Pierce and J. G. Wacker, hep-ph/0605162.
- [11] R. Bernabei *et al.* [DAMA Collaboration], Eur. Phys. J. C **56**, 333 (2008) [arXiv:0804.2741 [astro-ph]]; Eur. Phys. J. C **67**, 39 (2010) [arXiv:1002.1028 [astro-ph.GA]].
- [12] C. E. Aalseth *et al.* [CoGeNT Collaboration], Phys. Rev. Lett. **106**, 131301 (2011) [arXiv:1002.4703 [astro-ph.CO]]; Phys. Rev. Lett. **107**, 141301 (2011) [arXiv:1106.0650 [astro-ph.CO]].
- [13] G. Angloher *et al.* [CRESST-II Collaboration], Eur. Phys. J. C **72**, 1971 (2012) arXiv:1109.0702 [astro-ph.CO].
- [14] R. Agnese *et al.* [CDMS Collaboration], Submitted to Phys.Rev.Lett. [arXiv:1304.4279 [hep-ex]].
- [15] P. Draper, T. Liu, C. E. M. Wagner, L. -T. Wang, H. Zhang, Phys. Rev. Lett. **106**, 121805 (2011).
- [16] J. Kozaczuk and S. Profumo, arXiv:1308.5705 [hep-ph].
- [17] J. R. Ellis, J. F. Gunion, H. E. Haber, L. Roszkowski and F. Zwirner, Phys. Rev. D **39**, 844 (1989).
- [18] C. Panagiotakopoulos and K. Tamvakis, Phys. Lett. B **469**, 145 (1999) [arXiv:hep-ph/9908351].
- [19] V. Barger, P. Langacker, H. -S. Lee and G. Shaughnessy, Phys. Rev. D **73**, 115010 (2006) [hep-ph/0603247].
- [20] J. Shu and Y. Zhang, arXiv:1304.0773 [hep-ph].
- [21] U. Ellwanger, J. F. Gunion and C. Hugonie, JHEP **0502**, 066 (2005) [hep-ph/0406215]; U. Ellwanger and C. Hugonie, Comput. Phys. Commun. **175**, 290 (2006) [hep-ph/0508022]; G. Belanger, F. Boudjema, C. Hugonie, A. Pukhov and A. Semenov, JCAP **0509**, 001 (2005) [hep-ph/0505142]; U. Ellwanger and C. Hugonie, Comput. Phys. Commun. **177**, 399 (2007) [hep-ph/0612134]; M. Muhlleitner, A. Djouadi and Y. Mambri, Comput. Phys. Commun. **168**, 46 (2005) [hep-ph/0311167]; D. Das, U. Ellwanger and A. M. Teixeira, Comput. Phys. Commun. **183**, 774 (2012) [arXiv:1106.5633 [hep-ph]].
- [22] J. Huang, T. Liu, L. -T. Wang and F. Yu, in preparation.
- [23] J. Alwall, M. Herquet, F. Maltoni, O. Mattelaer and T. Stelzer, “MadGraph 5 : Going Beyond,” JHEP **1106**, 128 (2011) [arXiv:1106.0522 [hep-ph]].
- [24] J. Pumplin, D. R. Stump, J. Huston, H. L. Lai, P. M. Nadolsky and W. K. Tung, “New generation of parton distributions with uncertainties from global QCD analysis,” JHEP **0207**, 012 (2002) [hep-ph/0201195].
- [25] M. L. Mangano, M. Moretti and R. Pittau, Nucl. Phys. B **632**, 343 (2002) [hep-ph/0108069].
- [26] M. L. Mangano, M. Moretti, F. Piccinini, R. Pittau and A. D. Polosa, JHEP **0307**, 001 (2003) [hep-ph/0206293].
- [27] T. Sjostrand, S. Mrenna and P. Z. Skands, “PYTHIA 6.4 Physics and Manual,” JHEP **0605**, 026 (2006) [hep-ph/0603175].
- [28] J. Conway *et al.*, “Pretty Good Simulation of high energy collisions”, <http://physics.ucdavis.edu/~conway/research/software/pgs/pgs4-general.htm>
- [29] S. Chatrchyan *et al.* [CMS Collaboration], JINST **6**, P11002 (2011) [arXiv:1107.4277 [physics.ins-det]].
- [30] G. Aad *et al.* [ATLAS Collaboration], Eur. Phys. J. C **72**, 1909 (2012) [arXiv:1110.3174 [hep-ex]].
- [31] [ATLAS Collaboration], ATLAS-CONF-2011-063.
- [32] S. Chatrchyan *et al.* [CMS Collaboration], JINST **6**, P09001 (2011) [arXiv:1106.5048 [physics.ins-det]].
- [33] G. Aad *et al.* [ATLAS Collaboration], Phys. Lett. B **721**, 32 (2013) [arXiv:1210.0435 [hep-ex]].
- [34] G. Aad *et al.* [ATLAS Collaboration], Phys. Lett. B **719**, 299 (2013) [arXiv:1212.5409 [hep-ex]].
- [35] G. Aad *et al.* [ATLAS Collaboration], New J. Phys. **15**, 043009 (2013) [arXiv:1302.4403 [hep-ex]].
- [36] S. Chatrchyan *et al.* [CMS Collaboration], JHEP **1107**, 098 (2011) [arXiv:1106.2375 [hep-ex]].
- [37] J. F. Gunion *et al.*, “The Higgs Hunter’s Guide,” PERSEUS PUBLISHING (1990), Cambridge, Massachusetts.
- [38] D. Curtin, R. Essig, S. Gori, P. Jaiswal, A. Katz and T. Liu *et al.*, arXiv:1312.4992 [hep-ph], submitted to Phys. Rev. D.
- [39] J. M. Butterworth *et al.*, Phys. Rev. Lett. **100**, 242001 (2008). [arXiv:0802.2470 [hep-ph]].
- [40] G. D. Kribs, A. Martin, T. S. Roy and M. Spannowsky, Phys. Rev. D **82**, 095012 (2010) [arXiv:1006.1656 [hep-ph]].
- [41] G. D. Kribs, A. Martin, T. S. Roy and M. Spannowsky, Phys. Rev. D **81**, 111501 (2010) [arXiv:0912.4731 [hep-ph]].
- [42] Y. L. Dokshitzer, G. D. Leder, S. Moretti and B. R. Webber, JHEP **9708**, 001 (1997) [hep-ph/9707323].
- [43] M. Wobisch and T. Wengler, In *Hamburg 1998/1999, Monte Carlo generators for HERA physics* 270-279 [hep-ph/9907280].
- [44] M. Cacciari, G. P. Salam and G. Soyez, Eur. Phys. J. C **72** (2012) 1896 [arXiv:1111.6097 [hep-ph]].
- [45] R. Bonciani, S. Catani, M. L. Mangano and P. Nason, Nucl. Phys. B **529**, 424 (1998) [Erratum-ibid. B **803**, 234 (2008)] [hep-ph/9801375].
- [46] S. Dittmaier *et al.* [LHC Higgs Cross Section Working Group Collaboration], arXiv:1101.0593 [hep-ph].
- [47] J. Cao, F. Ding, C. Han, J. M. Yang and J. Zhu, JHEP **1311**, 018 (2013) [arXiv:1309.4939 [hep-ph]].
- [48] M. L. Graesser, Phys. Rev. D **76**, 075006 (2007) [arXiv:0704.0438 [hep-ph]].
- [49] J. Kersten and A. Y. Smirnov, Phys. Rev. D **76**, 073005 (2007) [arXiv:0705.3221 [hep-ph]].
- [50] A. de Gouvea, arXiv:0706.1732 [hep-ph].
- [51] C. Englert, M. Spannowsky and C. Wymant, Phys. Lett. B **718**, 538 (2012) [arXiv:1209.0494 [hep-ph]].